ChemComm

COMMUNICATION

Membrane-less organic-inorganic aqueous flow batteries with improved cell potential

Received 00th January 20xx,
Accepted 00th January 20xx

DOI: 10.1039/x0xx00000x

www.rsc.org/

P.K. Leung[a,b], T. Martin[a], A.A. Shah[c,d], M.A. Anderson[a], J. Palma[a]

A membrane-less organic-inorganic flow battery based on zinc and quinone species is proposed. By virtue of the slow dissolution rate of the deposited anode (< 11.5 mg h^{-1} cm^{-2}), the battery has a cell voltage of *c.a.* 1.52 V with an average energy efficiency of *c.a.* 73 % at 30 mA cm^{-2} over 12 cycles.

Redox flow batteries have been investigated extensively for mid- to large-scale applications, including grid-scale (up to MW/ MWh)[1 – 4]. For such applications, the technology possesses advantages over conventional energy storage systems in that these devices are not reliant on geological or geographical factors and are not disruptive to the environment, in contrast to pumped hydroelectric storage (PHS) or compressed air storage (CAS). They are also lower cost at large scales as well as safer compared to conventional batteries[1 – 4]. However, the capital cost of the conventional vanadium redox flow battery (> USD$ 220 / kWh) is still too high for extensive market penetration due to the use of expensive active materials (vanadium: *c.a.* USD$ 25 Kg^{-1}) and ion-exchange membranes (Nafion® 117: *c.a.* USD$ 250 m^{-2}). The costs of the active materials and separators contribute up to 30 % and 40 %, respectively, of the overall capital cost[5].

Several membrane-less flow battery systems have been proposed, including the soluble lead acid[6], zinc-nickel[7], copper-lead dioxide[8], cadmium-choranil[9], zinc-lead-dioxide[10] and zinc-cerium[11] systems. Many of these systems involve electrodeposition at one or both of their electrodes and take advantage of the slow dissolution of the deposited metals in the presence of active species in the common electrolytes. In some chemistries, the capacities of the batteries are still limited by the positive electrode reactions, since solid-phase transformations are involved within the electrode materials (i.e. PbO_2/ $PbSO_4$, NiOOH/ $Ni(OH)_2$)[6-10].

In our proposed membrane-less configuration, we use soluble active species for both electrode reactions and ensure that the dissolution of the deposited anode is sufficiently slow in the presence of the oxidized catholyte species. Metallic zinc and organic quinone are used as the active materials in this work due to their low-cost (< USD$ 8 Kg^{-1}), abundancy, reversibility (for flow battery applications)[11-13] and the resulting high electrode potentials in aqueous electrolytes. Facilitated by prior computational screening[12], benzoquinone compounds as the parent isomers were reported to have higher solubilities and to lead to more positive electrode potentials than naphthoquinone and anthraquinone counterparts. In fact, 1,4-benzoquinone is the prototypical member of the quinone family. Together with 1,2-benzoquinone, the molecular formula is $C_6H_4O_2$. Cyclic conjugation for these two benzoquinones are discontinuous and continuous, respectively. In comparison, 1,4-benzoquinone (Solubility: *c.a.* 0.1 M) is more stable and soluble than 1,2-benzoquinone (Solubility: *c.a.* 0.060 M). However, the reduced form of 1,2-benzoquinone (catechol, *c.a.* 3.9 M) is much more soluble than that of 1,4-benzoquinone (hydroquine, *c.a.* 0.6 M). With the incorporation of sulfonate functional groups (–SO_3H), the solubilities of both oxidized and reduced quinones can be up to 1.0 M [13]. More importantly, electrode potential is further shifted to +0.85 V *vs.* SHE, more positive than +0.65 V *vs.* SHE of 1,4-benzoquinone. The detailed experimental methods are described in the supplementary information. The resulting charging reactions are expressed as follows:

At the negative electrode, zinc(II) species is reduced to metallic zinc(0):

$$Zn^{2+} + 2\,e^- \leftrightarrow Zn \qquad E_0 = -0.76\ V\ vs.\ SHE \quad (1)$$

At the positive electrode, hydroquinone (HQ) species is oxidizied to benzoquinone molecules.

[a] IMDEA Energy, Mostoles, Madrid, 28935, Spain.
[b] Department of Materials, Oxford University, OX1 3PH, UK
[c] School of Engineering, University of Warwick, CV4 7AL, UK.
[d] Corresponding author: akeel.shah@warwick.ac.uk

Electronic Supplementary Information (ESI) available: [details of any supplementary information available should be included here]. See DOI: 10.1039/x0xx00000x

For 1,4-hydroquinone (hydroquinone):

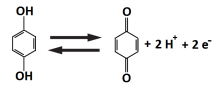

E_0 = +0.65 V *vs.* SHE (2)

For 1,2-hydroquinone (catechol):

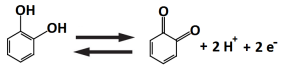

E_0 = +0.75 V *vs.* SHE (3)

For 1,2-hydroquinone-disulfonic acid:

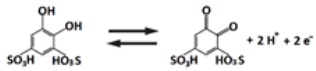

E_0 = +0.85 V *vs.* SHE (4)

In the charging process, hydrogen and oxygen evolutions are typical side reactions taking place at very negative and positive electrode potentials, respectively. Figure 1a shows the combined cyclic voltammograms of negative zinc and three types of positive quinone reactions (1,4-benzoquinone (1,4-BQ), 1,2-benzoquinone (1,2-BQ) and 1,2-benzoquinone-3,5 disulfonic acid (1,2-BQDS)), in which the measurements were made by sweeping the electrode potentials at 100 mV s^{-1}. It can be seen that the voltammograms of both electrode reactions were relatively reversible in terms of the peak separations and anodic/cathodic current density ratios. It can be seen that both hydrogen and oxygen evolutions (side reactions) are siginificant at pH 7 for the negative and positive electrode reactions.

For the case of 1,2-BQDS , the estimated cell voltage is as high as 1.65 V, which is comparable to the metallic all-vanadium redox flow batteries) However, these voltages tend to vary with the pH of the electrolytes. In order to identify the cell voltage range for typical operating conditions, the battery voltage was measured under a wide range of pH values (pH 1 – 12) (as shown in the E_0 *vs.* pH diagram of Figure 1b).

The estimated cell voltages were all higher than 1.45 V in this pH range (pH 1 – 12). For any of these molecules, the estimated cell voltages were all similar in acidic and neutral electrolytes (pH 1 – 8). As shown in Figure 1b, an increase in cell voltage is mainly observed in alkaline electrolytes (pH >8) due to the more negative electrode potential of the zinc electrode reaction. However, the electrochemical reduction of these benzoquinone species could lead to unstable species, such as semi-quinone (Q^{-}), quinone dianion (Q^{2-}) and the protonated anion (QH^{-}), which are less chemically stable compared to the hydroquinone (QH_2) obtained in acidic or neutral electrolytes[14].

Although acidic electrolytes also increase the overall cell voltages by shifting the electrode potentials of quinones towards more positive values, they also promote hydrogen evolution as a side reaction

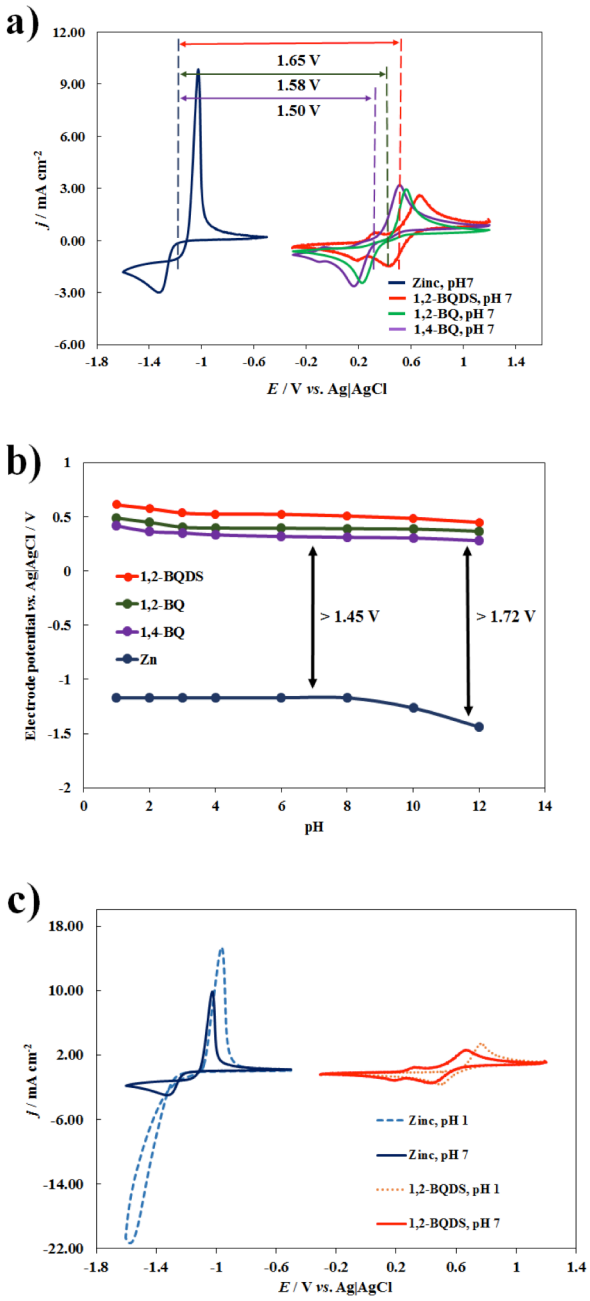

Figure 1. Electrochemical characteristics of zinc and hydroquinone molecules in 1 M sodium chloride solution: (a) combined cyclic voltammograms of zinc and hydroquinone molecules (1,2-HQDS, 1,2-HQ (catechol) and 1,4-HQ); (b) E_o vs. pH plots of zinc and hydroquinone molecules; (c) combined voltammograms of zinc and 1,2-HQDS at pHs 1 and 7; Potential sweep rate: 100 mV s^{-1}; electrolytes: 10 mM $ZnCl_2$ or hydroquinone in 1.0 M NaCl solution; substrate: glassy carbon electrode; room temperature.

(Figure 1c), leading to current efficiency of less than 30 % (anodic charge ÷ cathodic charge).

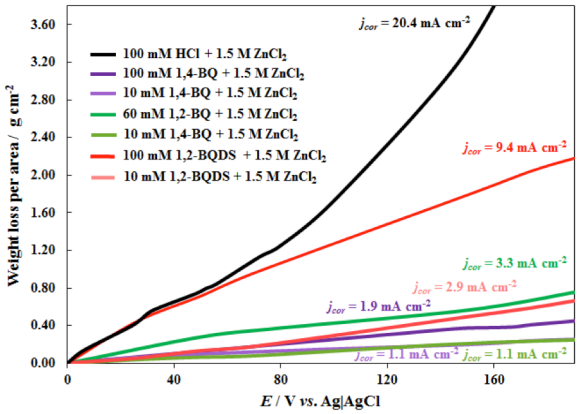

Figure 2. Effect of weight loss of metallic zinc samples under different electrolyte compositions ([HCl]/[1,4-BQ]/[1,2-BQ]/[1,2-BQDS], 1.5 M $ZnCl_2$ at pH 7) at room temperature. HCl concentration: 100 mM; Quinone concentrations: 10 or 100 mM (60 mM for 1,2-BQ due to its solubility limit); electrolyte volume: 100 cm^3.

Furthermore, the membrane-less concept in this work relies on the slow dissolution rate of the deposited anode species. In acidic electrolytes, metallic zinc reacts readily with protons and evolves hydrogen[15]. Thus, neutral electrolytes of pH 7 were used in the following tests. The use of this pH is to avoid the formation of various species and to ensure the only possible species at the end of the reactions are Zn, Zn^{2+}, Q, QH_2, as described in the relevant Pourbaix diagrams. In the absence of a separator, the charged benzoquinone species at the positive electrode are free to react with the metallic zinc at the negative electrode as a self-discharge process. In such a configuration, the dissolution of zinc caused by the direct reaction with benzoquinone species depends on the reaction kinetics and is limited by the surface area of the zinc anode exposed to the electrolyte. The rates of these reactions were evaluated by measuring the amount of zinc dissolved over time immersed in different electrolytes[15]. Figure 2 show the weight losses of the zinc samples in the presence of protons (100 mM) and oxidized benzoquinone species (10 or 100 mM; 60 mM for 1,2-BQ due to its solubility limit), representing a 100 % state-of-charge (SOC) as in the most adverse condition. It can be seen that the weight loss of zinc was much more significant in the acidic electrolyte (*c.a.* 25 mg h^{-1} cm^{-2}) compared to those with benzoquinones at pH 7 (< 11.5 mg h^{-1} cm^{-2}). This further shows that acidic electrolytes are not suitable for zinc-based membrane-less systems.

Regarding the three benzoquinone species, the weight losses of zinc samples was observed to be higher with 1,2-BQDS (< 11.5 mg h^{-1} cm^{-2}) than with the others (1,2-BQ: < 4.0 mg h^{-1} cm^{-2}; 1,4-BQ: < 2.4 mg h^{-1} cm^{-2}) . The resulting weight loss can be expressed as a form of corrosion current density by using Faraday's law (Figure 2). For the case of 1,2-BQDS, the corrosion current densities were between 2.9 and 9.4 mA cm^{-2} depending on the quinone concentrations (10 –

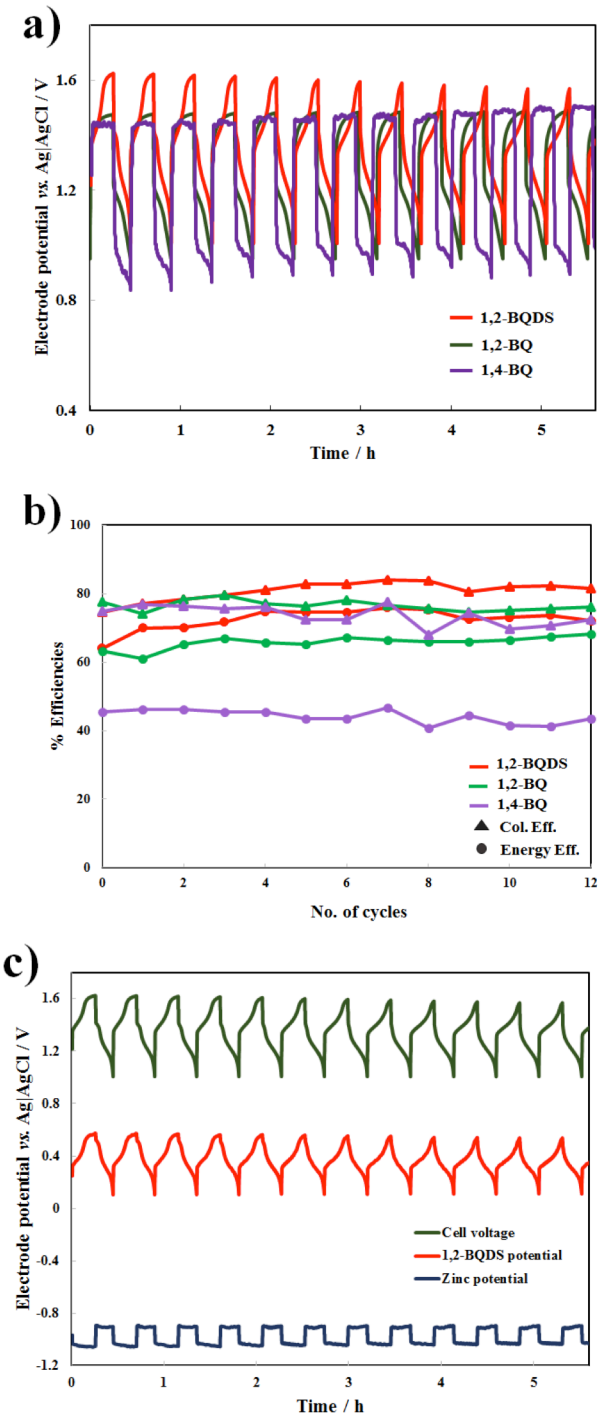

Figure 3. Cycling performance of a membraneless zinc-benzoquinone hybrid flow battery at 30 mA cm^{-2} and room temperature. (a) charge-discharge profiles of Zn/1,4-BQ, Zn/1,2-BQ and Zn/1,2-BQDS systems; (b) comparison of coulombic and energy efficiencies of the three battery systems; (c) half-cell electrode potential and overall cell voltages of the Zn/1,2-BQDS system. Electrolytes: 1.5 M $ZnCl_2$ and 50 mM hydroquinone; negative electrode: planar carbon; positive electrode: carbon felt; number of cycles: 12.

100 mM). Considering that metallic zinc is protected by the cathodic current during the charge process, the self-discharge of zinc mainly take place during discharge. As soon as benzoquinone is reduced back to the initial hydroquinone in the discharge process, the self-discharge process is expected to be slower towards a higher depth of discharge (DOD) (See Table S1 for the corresponding corrosion current densities in a 50 mM Zn/1,2-BQDS system) . Since these corrosion current densities (2.9 – 9.4 mA cm^{-2}) are still lower than the typical operating current densities used in redox flow batteries (≥ 30 mA cm^{-2}), this demonstrates the feasibility of using both zinc and 1,2-BQDS species in a membrane-less system.

The quinone species were further tested in a membrane-less parallel plate flow cell, in which carbon felt was used as the positive electrode material to facilitate the liquid-phase reactions. Similar to previous membrane-less systems, a concentrated zinc(II) electrolyte (1.5 M) was used to alleviate any mass transport limitations, and minimize the self-discharge of the zinc metal as reported in the previous work[15]. Figure 3a shows the charge-discharge profiles of the proposed chemistries using the three quinone molecules (1,4-BQ, 1,2-BQ and 1,2-BQDS) at 30 mA cm^{-2} over 12 cycles (15 min charge– 15 min discharge regime). The charge capacity is equivalent to an overall SOC of *c.a.* 55 % based on the energy content of the benzoquinone species. The coulombic and energy efficiencies were calculated and are summarized in Figure 3b. It can be seen that the coulombic efficiencies of these quinones were similar to each other (70 – 80 %), indicating that the self-discharge reactions between the deposited zinc and the benzoquinone species were not overwhelming in such experimental conditions (30 mA cm^{-2} and < *c.a.* 55 % SOC). Since the overall cell voltage were higher and lower voltage drops (between charge and discharge profiles) were observed, the voltage efficiency (1.24 V/ 1.54 V = *c.a.* 81 %) tends to be higher in the initial cycle than that of 1,4-BQ (0.88 V / 1.46 V = *c.a.* 61 %). The larger potential drop of 1,4-BQ (580 mV vs. 300 mV of 1,2-BQDS) is potentially due to the slower electron transfer kinetics in the relevant electrolyte conditions as suggested by the peak separations observed in the voltammograms (1,4-BQ: *c.a.* 350 mV; 1,2-BQDS: *c.a.* 250 mV) in Figure 1a (10 mM HQ, static electrolytes). After several cycles, the voltage efficiencies (i.e. *c.a.* 88 % in the 12th cycle) tended to increase, while those of the 1,4-BQDS decreased down to 60 %. Therefore, the average energy efficiency of 1,2-BQDS (*c.a.* 73 %) and 1,2-BQ (*c.a.* 66 %) are much higher than that of 1,4-BQ (*c.a.* 44 %) over the 12 cycles.

Figure 3c shows the resulting half-cell electrode potentials and the overall cell voltage of the zinc-1,2-BQDS systems during the charge-discharge process. This suggests that the voltage changes were mainly attributable to the polarization of the positive electrode, which is caused by the competing reactions between active species at the electrode surface, considering that the active concentration of 1,2-BQDS is much lower than that of metallic zinc ions (1.5 M) in the common electrolytes. The relatively low concentration of quinone species also leads to lower specific energy compared to the conventional systems. When higher quinone concentrations were used, lower coulombic efficiencies were observed in similar charge-discharge cycles (50 mM: η_{COL} = 74 %; 100 mM: η_{COL} = 62 %; 200 mM: η_{COL} = 24 %; See Figure S1). In the absence of separator, further increase in concentration is challenging but possible with the use of higher applied current densities, which can be facilitated by the improved mass transport and cell architecture. Furthermore, higher specific energy can be achieved readily with the use of separators, in which reversible reactions at high concentrations (i.e. 1.0 M) have been successfully demonstrated in previous works[11-13].

In summary, a membrane-less hybrid flow battery based on zinc and organic quinone species has been proposed and investigated from fundamental electrochemistry to the charge-discharge performance of the cell. With the use of 1,2-BQDS, a high operating voltage of *c.a.* 1.52 V was achieved, which is comparable to the conventional vanadium flow battery system (*c.a.* 1.3 V). Due to the low costs of the active materials, the overall electrolyte cost is less than USD$ 12 / kWh. In a common electrolyte containing oxidized quinone species, the slow dissolution of zinc means that a membrane-less configuration is feasible for the proposed chemistry. In the absence of separator, the capital cost of this battery could be less than the cost target of set by the US Department of Energy ($ 150 / kWh) and could be able to match existing physical energy storage technologies. This is a new direction for redox flow batteries and will promote the development of potentially low-cost and simpler alternatives to vanadium batteries for medium to large-scale energy storage.

References

1 M. Skyllas-Kazacos, M.H. Chakrabarti, S.A. Hajimolana, F.S. Mjalli, M. Saleem, *J. Electrochem. Soc.*, 2011, **158**, R55-R79.
2 J. Noack, N. Roznyatovskaya, T. Herr, P. Fischer, *Angew. Chem Int Ed*., 2015, **54**, 9776 – 9809.
3 C. Ponce de Leon, A. Frias-Ferrer, J. Gonzalez-Garcia, D.A. Szanto, F.C. Walsh, *J. Power Sources*, 2006, **160**, 716 – 732.
4 P. Leung, X. Li, C. Ponce de Leon, L. Berlouis, C.T.J. Low, F.C. Walsh, *RSC Adv.*, 2012, **2**, 10125-10156.
5 L. Joerissen, J. Garche, Ch. Fabjan, G. Tomazic, *J. Power Sources*, **127**, 2004, 98 -104.
6 D. Pletcher, R. Wills, *Phys. Chem. Chem. Phys*., 2004, **6**, 1779 – 1785.
7 Cheng, L. Zhang, Y-S. Yang, Y-H. Wen, G-P. Cao, X-D. Wang, *Electrochem. Communications*, 2007, **9**, 2639 – 2642.
8 J. Pan, Y. Sun, J. Cheng, Y. Wen, Y. Yang, P. Wan, *Electrochem. Communications,* 2008, **10**, 1226 – 1229.
9 Y. Xu, Y. Wen, J. Cheng, G.G.Y. Yang, *Electrochem. Communications,* 2009, **11**, 1422 - 1424.
10 P.K. Leung, Q. Xu, T.S. Zhao, *Electrochim. Acta*, 2012, **79**, 117 – 125.
11 P.K. Leung, C. Ponce de Leon, F.C. Walsh, *Electrochim. Acta*, 2012, **80**, 7 – 14.
12 S. Er, C. Suh, M.P. Marshak, A. Aspuru-Guzik, *Chem. Sci.,* 2015, **6**, 885-893.
13 B. Yang, L. Hoober-Burkhardt, S. Krishnamoorthy, A. Murali, G.K. Surya Prakash, S.R. Narayanan, *J. Electrochem. Soc.,* 2016, **163**, A1442 - A1449.
14 M. Quan, D. Sanchez, M.F. Wasylkiw, D.K. Smith, , *J. Am. Soc.,* 2007,**129**, 12847 - 12856.
15 P.K. Leung, C. Ponce de Leon, F.J. Recio, P. Herrasti, F.C. Walsh, *J. Appl. Electrochem*., 2014, **44**, 1025 – 1035.